Gyromagnetic Ratio of 2^+ Rotational States*

G. GOLDRING† AND R. P. SCHARENBERG
Physics Department and Laboratory for Nuclear Science, Massachusetts Institute of Technology, Cambridge, Massachusetts
(Received December 23, 1957)

The angular distribution of gamma rays following Coulomb excitation of millimicrosecond 2^+ states in Nd^{150}, Sm^{152}, Sm^{154}, Gd^{154}, Gd^{156}, and Gd^{160} were investigated. The gamma-ray angular distributions from solid oxide targets showed substantial perturbations. The attenuation coefficients for liquid nitrate targets were measured to be: Nd^{150}, $G_2{}^L=1\pm0.035$; Sm^{152}, $G_2{}^L=1\pm0.035$; Sm^{154}, $G_2{}^L=1.1\pm0.10$; Gd^{154}, $G_2{}^L=0.5\pm0.06$; Gd^{156}, $G_2{}^L=0.6\pm0.04$; Gd^{160}, $G_2{}^L=0.6\pm0.06$. The influence of the paramagnetic ion and the liquid environment on the angular distributions are discussed.

The effect of an external magnetic field (H_{ex}) on the unperturbed gamma-ray angular distribution from liquid targets was measured. The effect was attributed to the precession of the excited nucleus (gyromagnetic ratio g) in the external magnetic field that has been modified by the atomic structure (H_{eff}). For Nd^{150}, $H_{eff}=(2.3\pm0.3)H_{ex}$, $g=0.22\pm0.04$; Sm^{152}, $H_{eff}=(1.7\pm0.2)H_{ex}$, $g=0.21\pm0.04$; Sm^{154}, $H_{eff}=(1.7\pm0.2)H_{ex}$, $g=0.21\pm0.04$.

I. INTRODUCTION

THE purpose of this experiment was to measure the gyromagnetic ratio (g) of 2^+ states in even-even nuclei which are known as rotational states. This measurement is of interest because the gyromagnetic ratio will give direct information about the nature of the collective nuclear motion.

The nuclei investigated were even-even isotopes of neodymium, samarium, and gadolinium, which exhibit a fully developed rotational structure. These nuclei have 2^+ states of approximately 100-kev energy and lifetimes of about 10^{-9} sec. In this experiment, the collective nuclear state was Coulomb-excited, and the effect of a static magnetic field on the excited nucleus was detected by the change in the angular distribution of the de-excitation gamma radiation.

Protons incident on a target, Coulomb-excite a nucleus that subsequently de-excites by the emission of a gamma ray. For these measurements, the resultant gamma-ray angular distribution can be written,[1]

$$W(\theta)=1+G_2A_2P_2(\cos\theta)+G_4A_4P_4(\cos\theta),$$

where G_2 and G_4 are the attenuation factors that describe the effect of spin couplings between the nucleus and its environment. A_2 and A_4 are determined by the Coulomb excitation process, the nuclear spins involved, and the multipole order of gamma radiation. $P_2(\cos\theta)$ and $P_4(\cos\theta)$ are Legendre polynomials.

In these experiments, the Coulomb excitation conditions are chosen so that the A_4 coefficient is negligible. Hence, we write

$$W(\theta)=1+G_2A_2P_2(\cos\theta). \quad (1)$$

Because of the strong spin couplings in solids, the magnetic field measurements must be carried out with the nucleus in a liquid environment. We expect that, in a liquid environment, there will be an interaction between the quadrupole moment of the excited nucleus and randomly fluctuating electric-field gradients at the nucleus set up by neighboring atoms. In a liquid paramagnetic environment, we would also expect an interaction between the magnetic moment of the excited nucleus and randomly fluctuating magnetic fields set up by the paramagnetic ions. We shall denote the effect of such time-dependent interactions on the gamma-ray angular distributions by the attenuation factor $G_2{}^L$.

In the presence of such time-dependent interactions in a liquid and also in the presence of a static magnetic field H placed perpendicular to the plane of the beam and the gamma-ray counters, Eq. (1) becomes[1]

$$W(\theta,H)=1+\frac{G_2{}^LA_2}{4}+\frac{3G_2{}^LA_2}{4}\left(\frac{\cos2\theta+2\omega_L\tau_nG_2{}^L\sin2\theta}{1+(G_2{}^L2\omega_L\tau_n)^2}\right), \quad (2)$$

where τ_n is the mean lifetime of the excited nuclear state, $\omega_L=g\mu_nH/h$ is the Larmor frequency, $\mu_n=e\hbar/2m_pc$ the nuclear magneton, $G_2{}^L$ the attenuation factor associated with the time-dependent perturbation. For the conditions of this experiment, $\omega_L\tau_n\ll1$, Eq. (2) becomes

$$W(\theta,H)=1+\tfrac{1}{4}G_2{}^LA_2+\tfrac{3}{4}G_2{}^LA_2\cos2\theta+\tfrac{3}{2}\omega_L\tau_n(G_2{}^L)^2A_2\sin2\theta. \quad (3)$$

II. EXPERIMENTAL ARRANGEMENT

The experimental arrangement is shown in Fig. 1. The targets were bombarded by a 2.1-Mev proton beam from the M.I.T. Rockefeller electrostatic generator, and two gamma-ray counters were placed at $\pm\frac{3}{4}\pi$ with respect to the incident proton beam. The ratio of the counting rates of the two counters is measured for

* This work has been supported in part by the joint program of the Office of Naval Research and the U. S. Atomic Energy Commission.
† On leave of absence from the Weizmann Institute of Science, Rehovoth, Israel.
[1] A. Abragam and R. V. Pound, Phys. Rev. **92**, 943 (1953).

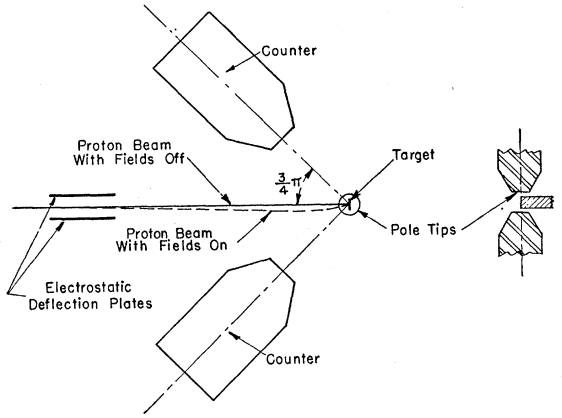

FIG. 1. Schematic drawing of experimental arrangement. (In the center of the figure, $3/4\pi$ should read $\pi/4$.)

magnetic field up and magnetic field down:

$$\frac{R(\uparrow)}{R(\downarrow)}=\left\{\frac{1+\frac{1}{4}G_2{}^L A_2+\frac{3}{2}\omega_L\tau_n(G_2{}^L)^2A_2}{1+\frac{1}{4}G_2{}^L A_2-\frac{3}{2}\omega_L\tau_n(G_2{}^L)^2A_2}\right\}^2$$

$$\cong 1+6(G_2{}^L)^2A_2\omega_L\tau_n. \quad (4)$$

To extract ω_L from this measurement, independent knowledge of $G_2{}^L$, A_2, and τ_n is required. For a 0^+ to 2^+ Coulomb excitation process, A_2 can be calculated accurately.[2] Measurement of the gamma-ray angular distribution then gives an independent value for $G_2{}^L$. Typical values for these experiments are $G_2{}^L=1$, $A_2=0.2$, $\omega_L\tau_n=0.05$. Thus, $R(\uparrow)/R(\downarrow)=1.06$. To measure the ratio $R(\uparrow)/R(\downarrow)$ to 0.1% requires 10^6 counts. This is feasible with the experimental arrangement.

The assembly of the magnetically shielded counters is shown in Fig. 2. The effectiveness of this design was checked by placing a Co^{57} source at the target position and observing the counting rate on the side of the 125-kev gamma photopeak for magnetic field up and magnetic field down. No shift in pulse height was observed.

The electronic equipment consisted of standard 2-megacycle amplifiers and single-channel analyzers (Model 500 Atomic Instrument Company) and was stable for indefinite periods.

The details of the target chamber are shown in Fig. 3. The magnetic fringe field bends and deflects the proton beam, changing the incident proton direction and the solid angles subtended by the counters. To minimize these effects, the area of the magnetic field was made as small as possible, and the beam was magnetically shielded.

The electrostatic deflection plates were introduced 50 cm from the target to eliminate completely the small (about 2 mm) residual beam deflection. To determine the electrostatic voltage correctly, the proton beam of diameter 1 mm was swept electrostatically across a point palladium target, and the palladium x-rays were recorded. This measurement was repeated with the magnetic field turned on. The displacement of the two beam profiles obtained in this way gives the correct electrostatic deflection voltage. The effect of the proton beam displacement on the ratio $R(\uparrow)/R(\downarrow)$ was reduced to $R(\uparrow)/R(\downarrow)=1\pm0.002$ by this method. This is equivalent to a beam displacement uncertainty of ±0.1 mm.

The beam bending was measured in two ways:

1. The magnetic field was measured along the proton beam path, using a Hall-effect probe[3] calibrated against a nuclear resonance meter and the beam-bending angle was computed to be $\Delta\theta_p=0.0834$ radian.

2. The short-lived unresolved states near 313 kev in Ag^{107} and Ag^{109} were excited. The ratio $R(\uparrow)/R(\downarrow)$ and the angular distribution of the gamma radiation were measured. Because of the short lifetime, the effect of the precession is negligible. The value of the angle of the beam bending measured in this way, $\Delta\theta_p=0.0829\pm0.0015$, is in excellent agreement with the above field-integration value.

These measurements also served to determine the value of the applied magnetic field H at the target spot.

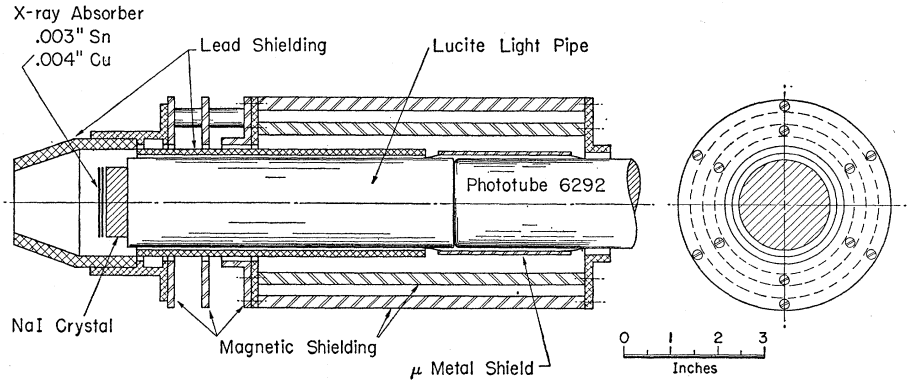

FIG. 2. Counter assembly and shielding.

[2] Alder, Bohr, Huus, Mottelson, and Winther, Revs. Modern Phys. 28, 432 (1956).
[3] Model D-79, Dyna-Empire Company, Garden City, New York.

$H=16\,000\pm300$ gauss. A survey of the magnetic field at the target spot showed that the magnetic field was homogeneous to $\pm2\%$ in a cube 2 mm on a side.

III. SOLID TARGETS

A preliminary investigation of the angular distribution of the gamma radiation from thick solid targets was carried out. The targets consisted of 20 mg of the separated isotope oxide pressed on a $\frac{1}{4}$-in. diameter tin disk. A typical spectrum is shown in Fig. 4. The background radiation is about 1/20 of the gamma-ray intensity at the photopeak. Measurements of the angular distribution of the background were carried out for thick metallic tin and lead targets at several photon energies. The intensity, energy spectrum, and angular distribution of the radiation are in agreement with those expected for proton bremsstrahlung. For example, when lead is bombarded with 2.1-Mev protons, the 125-kev radiation has an angular distribution $W(\theta)=1-(0.22\pm0.025)P_2(\cos\theta)$ which compares with the calculated value[2] of $A_2=-0.22$.

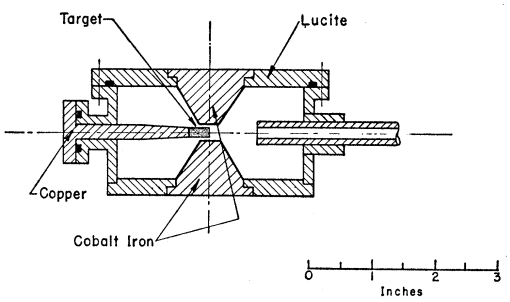

FIG. 3. Details of the target chamber.

The measured angular-distribution coefficients corrected for proton bremsstrahlung background are compared with the theoretical values in Table I. Substantial perturbations are evident.

IV. LIQUID TARGETS

The development of a suitable liquid target was the principal experimental problem. The target requirements are (a) a highly soluble compound, or melt, which is chemically stable under proton bombardment; (b) a stable proton window; (c) a nonmagnetic container, which can conduct the heat away and will resist chemical attack; and (d) a design that will permit the use of small (approximately 30 mg) amounts of separated isotopes.

The nonviscous liquids adopted, which proved to be entirely satisfactory, were aqueous solutions of the rare-earth nitrates in excess nitric acid. The concentration of the solutions was 400 grams/liter. Thin (1 mg/cm^2) quartz proved to be a superb window material, through which the liquid behavior could be monitored. The beam position was also continuously visible because of the fluorescence of the quartz. The

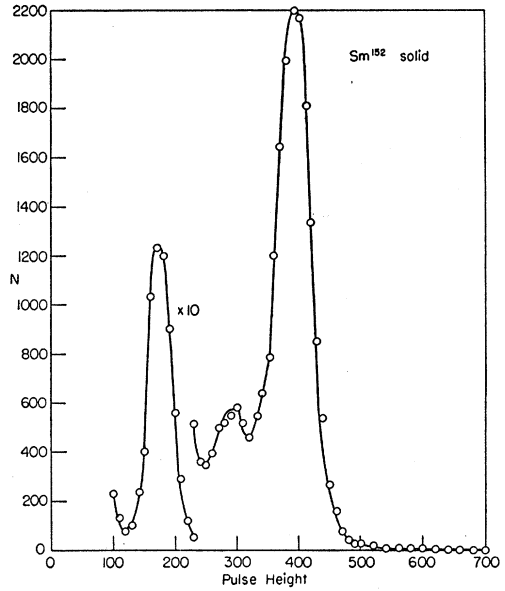

FIG. 4. Gamma spectrum from solid oxide target of Sm^{152}. Counts are normalized arbitrarily.

body of the target was made of completely annealed nonmagnetic stainless steel (Ryerson No. 202). A satisfactory design was evolved to remove the gases formed by proton ionization without disturbing the liquid layer next to the window. A detailed description of the target technique will be given elsewhere.

V. LIQUID-TARGET ANGULAR-DISTRIBUTION MEASUREMENTS

A standard procedure was used in measuring the liquid-target angular distributions. (a) The face of the target, which was inclined at 20 degrees with respect to the direction of the proton beam, was accurately positioned with a telescope. (b) The x-ray and gamma-ray counts were recorded for the movable counter for eleven points between 80 and 30 degrees. (c) The measurements were normalized to the x-ray counts in the fixed counter. (d) The beam position was monitored using a telescope. (e) The value of A_2 obtained by a least-squares fit to the data was corrected for the finite angular resolution ($\sigma=0.021$ of 4π) of the movable counter. (f) The measured value of A_2 was corrected for background. (g) As a check on scattering, the x-ray angular distributions were measured and found to be isotropic.

TABLE I. Angular-distribution measurements from solid oxide $(X)_2O_3$ targets.

Nucleus	A_2(theoretical)	A_2(experimental)	G_2
Nd^{150}	0.191	0.067 ± 0.005	0.35 ± 0.03
Sm^{152}	0.187	0.114 ± 0.005	0.61 ± 0.03
Sm^{154}	0.143	0.076 ± 0.005	0.53 ± 0.03
Gd^{156}	0.145	0.041 ± 0.005	0.28 ± 0.03

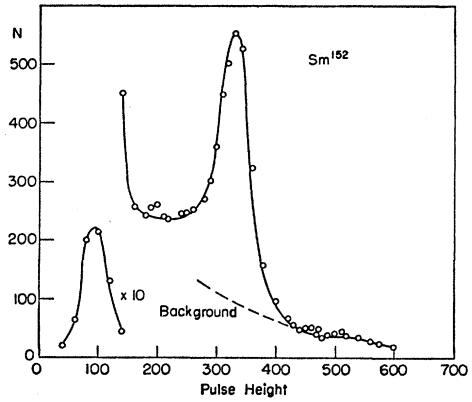

FIG. 5. Gamma spectrum from liquid Sm^{152} target. Counts are normalized arbitrarily.

Figure 5 shows a typical spectrum from a liquid target. As a comparison, a spectrum of the same nucleus is shown in Fig. 4, when it is bombarded in solid oxide form. The ratio of the gamma-ray intensities from the two targets is about 1:15.

In these targets, the ratio of the gamma-ray counting rate to the background counting rate at the photopeak is between 3 and 5. To establish the spectrum and angular distribution of the background, targets consisting of similar solutions of $La(NO_3)_3$ and $Pb(NO_3)_2$ were investigated. The spectra were found to be essentially identical so that the background spectrum could be accurately extrapolated for any given case. A background spectrum derived in this way is shown in Fig. 5. The angular distribution was also found to be similar for $La(NO_3)_3$ and $Pb(NO_3)_2$ liquid targets. For example, photons of 125 kev had an angular distribution of $1+A_2P_2(\cos\theta)$ with $A_2=-0.155\pm0.006$ for La and $A_2=-0.19\pm0.008$ for Pb. The angular distributions of the radiation from a $La(NO_3)_3$ liquid target is shown in Fig. 6 for two photon energies.

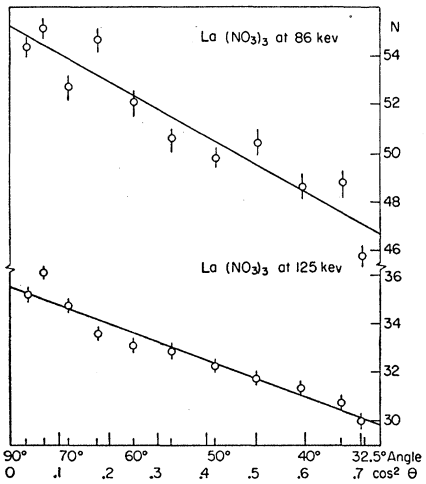

FIG. 6. Angular distribution of radiation from liquid La target at 85 and 125 kev.

In the present work, as in all electric excitation work concerned with gamma radiation, the bremsstrahlung background is a necessary evil; however, in our case, it also has one advantage: it reduces the effect of the beam turning on the ratio $R(\uparrow)/R(\downarrow)$. The precession is related to the angular distribution of the gamma rays, whereas the beam turning will depend on the A_2 of the over-all angular distribution. Since the A_2 of the background is negative and quite large, the over-all A_2 will be somewhat smaller than the A_2 of the gamma transition. The results of the angular-distribution measurements are given in Table II. A typical distribution is shown in Fig. 7.

VI. INTERPRETATION OF LIQUID-TARGET RESULTS

The gamma-ray angular distributions from Nd^{150}, Sm^{152}, and Sm^{154} are essentially unperturbed, in contrast with the solid oxide target results which exhibited substantial perturbations. These are further examples of a liquid environment restoring a correlation perturbed in solid environment. Since Nd^{3+} and Sm^{3+} are paramagnetic ions, the perturbing interaction in the solid could be either an electric or a magnetic interaction

TABLE II. Angular distributions from liquid targets.

Nucleus	A_2(calculated)	A_2(experimental)	$G_2{}^L$
Nd^{150}	0.191	0.192±0.006	1 ±0.035
Sm^{152}	0.187	0.189±0.006	1 ±0.035
Sm^{154}	0.143	0.156±0.015	1.1±0.10
Gd^{154}	0.199	0.10 ±0.012	0.5±0.06
Gd^{156}	0.145	0.087±0.006	0.6±0.04
Gd^{160}	0.143	0.09 ±0.01	0.6±0.06

or both. In any event, the effect of an electric or magnetic interaction in the liquid environment is small. Since the electric environment (neighboring water molecules) is essentially the same for the Gd isotopes, we would expect that the Gd angular distributions are not appreciably perturbed by a time-dependent quadrupole interaction. The angular distributions of the Gd isotopes show substantial perturbation, but it is noticeably less than that observed from the solid oxide targets. The magnitude of the perturbation is approximately the same for these three Gd isotopes. If only a time-dependent quadrupole interaction between the quadrupole moment of the excited state and the electric field gradient at the nucleus is involved, then

$$G_2{}^L=(1+\lambda_2\tau_n)^{-1},$$

where

$$\lambda_2\tau_n\propto\left\langle\left(\frac{eQ}{\hbar}\right)^2\left(\frac{\partial^2V}{\partial z^2}\right)^2\right\rangle_{\text{Av}}\tau_c\tau_n. \tag{5}$$

Since the electric environment is identical for the isotopes, it is possible to estimate the relative values of $\lambda_2\tau_n$ for the Gd isotopes by using the Coulomb excita-

tion data, $B(E2)$ values, gamma-ray energy, and the value of the $E2$ internal-conversion coefficients. For example,

$$(\lambda_2\tau_n)_{Gd^{160}}/(\lambda_2\tau_n)_{Gd^{154}}=3.$$

This effect is certainly not observed.

The magnitude of the perturbation of the Gd gamma angular distributions is in agreement with that expected for a static magnetic interaction between the Gd^{3+} ion and the magnetic moment of the excited 2^+ state.

The results of recent paramagnetic-resonance experiments show that Gd^{3+} has a small hyperfine interaction.[4] Gd^{3+} has $(4f)^7$ electrons, a half-filled shell. The ground state is an $^8S_{7/2}$ level. No magnetic hyperfine interaction is expected for an ion in this state. Low attributes the measured value to unpaired s electrons resulting from configurational interaction. This hyperfine structure is expected to be only slightly dependent on the crystalline environment. According to Alder,[5] the effect of an $A(\mathbf{I}\cdot\mathbf{J})=\hbar\omega_s(\mathbf{I}\cdot\mathbf{J})$ interaction on the gamma-ray

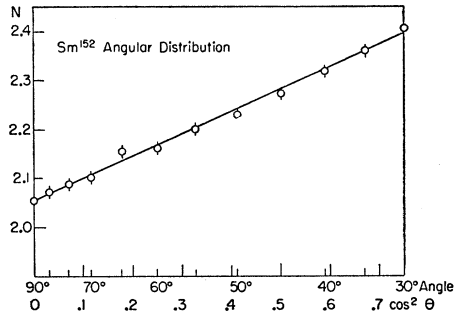

FIG. 7. Over-all angular distribution of gamma radiation and background from liquid Sm^{152} target.

angular distribution is given by

$$G_2{}^L=\sum_{FF'}\frac{(2F+1)(2F'+1)|W(IJ2F|F'2)|}{1+(\omega_{FF'}\tau_n)^2},$$

where $\mathbf{F}=\mathbf{I}+\mathbf{J}$, $\hbar\omega_{FF'}=\frac{1}{2}A\{F(F+1)-I(I+1)-J(J+1)\}$, and τ_n is the mean life of the excited nuclear state. We can estimate $A/g\mu_n$ from Low's value for Gd^{157} and the known value of the Gd^{157} magnetic moment.

The lifetime of the excited 2^+ state in Gd^{154} has been measured by Sunyar.[6] The Gd^{156} and Gd^{160} lifetimes have been estimated by using the Gd^{154} lifetime as a basis, and the Coulomb excitation data given in reference 2. The attenuation coefficients are computed for two values of the gyromagnetic ratio of the excited 2^+ state. The measured attenuation coefficients are compared with the computed values in Table III. The calculated values are uncertain because of the 10% uncertainty in the Gd^{157} moment[4] and a 15% uncertainty in the lifetime of the excited state. However,

[4] W. Low, Phys. Rev. **103**, 1309 (1956).
[5] K. Alder, Helv. Phys. Acta **25**, 235 (1953).
[6] A. W. Sunyar, Phys. Rev. **98**, 653 (1955).

TABLE III. Comparison of measured and calculated values of the attenuation coefficients $G_2{}^L$ for the Gd isotopes.

Nucleus	Energy (kev)	τ_n (sec)[a]	$G_2{}^L$ (experimental)	$G_2{}^L$ (computed) ($g=0.2$)	($g=0.4$)
Gd^{154}	124	$(1.70\pm0.14)\times10^{-9}$	0.5 ± 0.06	0.62	0.47
Gd^{156}	90	$[\sim2\times10^{-9}]$	0.6 ± 0.06	0.57	0.39
Gd^{160}	76	$[\sim2\times10^{-9}]$	0.6 ± 0.06	0.57	0.39

[a] The mean lives in square brackets are estimated values.

the measured perturbations are consistent with those expected for a static $A(\mathbf{I}\cdot\mathbf{J})$ interaction between the Gd^{3+} ion and a magnetic moment whose magnitude is between 0.4 and 0.8 nuclear magneton.

In contrast with the Gd angular distributions, the angular distributions of the gamma rays from Nd^{150}, Sm^{152}, and Sm^{154}, within the accuracy of the measurements, are unperturbed. This result is unexpected because of the large magnetic hyperfine interaction known to exist between the Nd^{3+} and Sm^{3+} ions and the nuclei. The unperturbed gamma angular distributions are the consequence of the extremely short paramagnetic relaxation time of the Nd^{3+} and Sm^{3+} ions in a liquid environment at room temperature.

The results of paramagnetic-resonance experiments on Nd^{3+} and Sm^{3+} show that such a strong magnetic hyperfine interaction exists[7] ($A=0.006$ cm^{-1}). This interaction corresponds to a magnetic field at the nucleus of order 10^6 gauss; i.e., $\omega_s\tau_n\geq1$. If the electron shell were in a stationary state for a time $\tau_s\gg\tau_n$, a considerable perturbation would be observed. If the electronic paramagnetic-relaxation time is very much less than the nuclear lifetime $\tau_s\ll\tau_n$, then the effect of the hyperfine interaction on the gamma-ray angular distribution can be removed. Abragam and Pound[1] show that

$$G_2{}^L=(1+\lambda_2{}^L\tau_n)^{-1},$$

where

$$\lambda_2{}^L\tau_n\propto\omega_s\tau_s\tau_n.$$

We can estimate the paramagnetic-relaxation time if we assume the g-factor of the excited state to be the same as that of the odd-A isotope, Sm^{153} ($A=0.006$ cm^{-1}, $J=\frac{5}{2}$). For Sm^{152}, $G_2{}^L=1\pm0.035$, the paramagnetic relaxation time τ_s must be of order 8×10^{-13} sec to account for the unperturbed result.

Therefore, the difference between the Gd^{3+} case and the Nd^{3+} and Sm^{3+} cases is due to the difference in paramagnetic-relaxation times. Because Gd^{3+} is an S state, $\mathbf{J}=\mathbf{S}$ is not coupled to the lattice via the spin-orbit coupling. Sm^{3+}, on the other hand, has an unfilled $(4f)^5$ shell. The ground level is an $H_{\frac{5}{2}}$ state, which should strongly couple to the liquid environment.

VII. MAGNETIC FIELD EXPERIMENTS

The g-factor runs were interlaced with the angular distribution runs. A typical combined g-factor and

[7] R. J. Elliott and K. W. H. Stevens, Proc. Roy. Soc. (London) **A219**, 387 (1953).

TABLE IV. Magnetic-field experiment results.

Nucleus	Energy (kev)	$\omega_L\tau_n$	$g\tau_n$ (sec)	τ_n (sec)[a]	g
Nd^{150}	130	0.0945 ± 0.005	5.3×10^{-10}	$[2.38\times10^{-9}]$	$+0.22\pm0.04$
Sm^{152}	125	0.0568 ± 0.004	4.2×10^{-10}	$(2.02\pm0.14)\times10^{-9}$	$+0.21\pm0.04$
Sm^{154}	84	0.110 ± 0.008	8.0×10^{-10}	$[3.80\times10^{-9}]$	$+0.21\pm0.04$

[a] The mean lives in square brackets are estimated values.

angular distribution run, using a single target, would last about 10 hours. Energy spectra were taken at the beginning and the end of the run. No change in the liquid-target spectrum was observed. The number of gamma rays recorded per microcoulomb of the proton beam were used as a further index of target performance. Because of the large differences in this ratio between liquid and solid targets (a factor of 15), precipitation of the solute would be immediately obvious.

The g-factor measurements were made alternating the magnetic field direction about every minute. The value of $R(\uparrow)/R(\downarrow)$ obtained in this way is corrected for the beam-turning effect and for background. To interpret this corrected value of the ratio $R(\uparrow)/R(\downarrow)$, we assumed $G_2{}^L\equiv1$ and used the theoretical value of A_2 as suggested by the results of the liquid-target measurements. The values of $\omega_L\tau_n$ obtained in this way are shown in Table IV. To obtain the gyromagnetic ratio, the value of the effective magnetic field at the nucleus must be computed.

The external magnetic field is modified by the atomic structure. Both Nd and Sm are strongly paramagnetic, and for any given orientation of the atom (i.e., fixed value of J_z), fields of the order of 10^6 gauss are produced at the nucleus. In the absence of an external field, this field averages out to zero during the lifetime of the excited nucleus because the atom changes its orientation in a random manner within a time that is small compared with the nuclear half-life. When an external field is applied, the atomic levels belonging to $+J_z$ and $-J_z$ are split, and the thermal equilibrium under these conditions implies a nonequal population for the $+J_z$ and $-J_z$ states. The excess population in one group of levels will produce a finite mean field at the nucleus. The process is very similar to the ordinary atomic polarization; and, in fact, the atomic field at the nucleus is a localized manifestation of the field pattern, the spatial average of which produces the atomic susceptibility.

To evaluate the field at the nucleus, we write the interaction of the nucleus with external fields as

$$H_1=\mu_n g_n(\mathbf{H}\cdot\mathbf{I})+A(\mathbf{J}\cdot\mathbf{I}),$$

where $\mathbf{J}$ is the atomic angular momentum and A is a constant related to the hyperfine splitting. $\mathbf{H}\equiv\mathbf{H}_{ex}$ is the applied magnetic field.

The mean value of H_1 for a given value of I_z (where the z axis is in the direction of $\mathbf{H}$) but averaged over the atomic states is given by

$$\bar{H}_1=\mu_n g_n H I_z+A\bar{J}_z I_z,$$

where $\bar{J}_z$ is the mean value of J_z.

The atomic susceptibility is given by[8]

$$\chi_0=N\mu_e g_e\bar{J}_z/H,$$

where N is the number of atoms per cc and

$$g_e=1+\frac{S(S+1)+J(J+1)-L(L+1)}{2J(J+1)}.$$

We therefore have

$$\bar{H}_1=\mu_n g_n I_z H\left(1+\frac{A\chi_0}{N\mu_e\mu_n g_e g_n}\right).$$

In reference 8, a g_{eff} is defined by

$$\chi_0=N\mu_e{}^2 g_{\text{eff}}{}^2/3kT.$$

In terms of g_{eff}, we have

$$H_1=\mu_n g_n I_z H\left(1+\frac{\mu_e}{\mu_n}\frac{A}{2kT}\frac{g_{\text{eff}}{}^2}{g_e g_n}\right).$$

This may be interpreted as an interaction of the nucleus with an effective field:

$$H_{\text{eff}}=H\left(1+\frac{\mu_e}{\mu_n}\frac{A}{3kT}\frac{g_{\text{eff}}{}^2}{g_e g_n}\right).$$

Strictly speaking, A and g_n refer to the excited 2^+ state in the even-even nucleus under investigation. However, A is proportional to g_n and, therefore, A/g_n will be the same for all levels of all the isotopes of that nucleus; e.g., the ground level of an odd-A isotope.

The values of A for odd-A isotopes may be computed from the paramagnetic hyperfine-structure data.[7] These values are $A=0.0076$ cm^{-1} for Nd^{3+} and $A=0.006$ cm^{-1} for Sm^{3+}. The values of g_n are also reported in that paper. From these, it will be seen that

$$H_{\text{eff}}=(2.3\pm0.3)H \quad \text{for } Nd^{3+},$$
$$H_{\text{eff}}=(1.7\pm0.2)H \quad \text{for } Sm^{3+}.$$

The error is due to the uncertainty in the values of g_n.

It is important to note the foregoing analysis is valid only if the atomic structure in the neighborhood of the decaying nucleus is in a state of thermal equilibrium at room temperature.

The recoiling ion of energy $\sim$50 kev travels in a straight line, leaving a tube of ions each with about $\sim$30-ev energy. The characteristic time for the temperature to decay by $1/e$ is given by $\alpha^2/6K$,[9] where K is the diffusivity of the material and α is the radial

[8] J. H. Van Vleck, *The Theory of Electric and Magnetic Susceptibilities* (Clarendon Press, Oxford, 1932).

[9] H. S. Carslaw and J. C. Jaeger, *Conduction of Heat in Solids* (Clarendon Press, Oxford, 1948), Chap. 7.

dimension of the cylindrical region. We can set an upper limit to the thermalization time by estimating the characteristic time when the region is close to room temperature; that is, when α is large. $\alpha \simeq 3\times10^{-7}$ cm corresponds to about four times room temperature. For water, $K=1.4\times10^{-3}$ cgs units. Thus $\tau_c \simeq 1\times10^{-11}$ sec. Hence, we conclude that the ion reaches thermal equilibrium at room temperature in a time short compared with $\tau_n=2\times10^{-9}$ sec.

VIII. g-FACTOR RESULTS

Sm^{152}, Sm^{154}.—The half-life of the 122-kev 2^+ state of Sm^{152} has been measured by Sunyar[6] to be $T_{\frac{1}{2}} = (1.4\pm0.1)\times10^{-9}$ sec. The ratio of the mean lives of the 84-kev 2^+ state in Sm^{154} to that of the 122-kev 2^+ state in Sm^{152} can be computed using the values of $B(E_2)$ and internal conversion coefficient given in reference 2. The computed mean life of the 84-kev 2^+ state in Sm^{154} is 3.80×10^{-9} sec. Using these mean lives, the observed value of the precession angle, and the effective value of the magnetic field H_{eff} for the Sm^{3+} ion, we extract the gyromagnetic ratio of the 2^+ states.

$$\text{122-kev } 2^+ \text{ state in } Sm^{152}: \quad g=+0.21\pm0.04,$$
$$\text{84-kev } 2^+ \text{ state in } Sm^{154}: \quad g=+0.21\pm0.04.$$

Nd^{150}.—The ratio of the mean lives of the 130-kev 2^+ state in Nd^{150} to that of the 122-kev 2^+ state in Sm^{152} can be computed using the values of $B(E_2)$ and internal conversion coefficient given in reference 2. The computed mean life of the 130-kev 2^+ state in Nd^{150} is 2.38×10^{-9} sec. Using this mean life, the effective value H_{eff} of the magnetic field for the Nd^{3+} ion, and the observed precession angle, we obtain the gyromagnetic ratio of the 2^+ state:

$$\text{130-kev } 2^+ \text{ state in } Nd^{150}, \quad g=0.22\pm0.04.$$

These results are summarized in Table IV.

IX. CONCLUSIONS

The gyromagnetic ratio of 2^+ states in Sm^{152}, Sm^{154}, and Nd^{150} are within 20% the same. The magnitude of the g-factor is near $+0.2$, assuming the conditions discussed previously. This value may be compared with the value $g'=Z/A=0.4$. The value Z/A results if the spins are coupled to zero and if the angular momentum is carried by a representative fraction of the nuclear matter.

The effect of a paramagnetic ion in a liquid environment on the gamma-ray angular distribution is shown to depend on whether the paramagnetic relaxation time is shorter or of the same order as the nuclear decay time. The magnitude of the perturbation of the gamma-ray angular distributions in the Gd isotopes is in agreement with that expected for a static magnetic interaction between the Gd^{3+} ion and the magnetic moment of the excited 2^+ state.

ACKNOWLEDGMENTS

The authors would like to thank Professor M. Deutsch for his continued interest in the problem. We should like to express our indebtedness to Dr. A. Abragam for his help in interpreting the results and for calculating the internal field correction. We should also like to thank Professor R. V. Pound and Professor A. Kerman for helpful discussions. Acknowledgment is also made of the assistance we received from Mr. Matti Salomaa in running the Rockefeller generator.